Optimization of $Al_2O_3:Er^{3+}$ waveguide technology for active integrated optical devices

Kerstin Wörhoff, Jonathan Bradley, Feridun Ay, Dimitri Geskus,
Tom Blauwendraat, and Markus Pollnau
Integrated Optical Microsystems Group, MESA+ Institute for Nanotechnology,
University of Twente, P.O. Box 217, 7500 AE Enschede, The Netherlands
e-mail: K.Worhoff@ewi.utwente.nl

ABSTRACT

Amorphous Al_2O_3 is a promising host material for active integrated optical applications such as tunable rare-earth-ion-doped laser and amplifier devices. The fabrication of slab and channel waveguides has been investigated and optimized by exploiting reactive co-sputtering and ICP reactive ion etching, respectively. The Al_2O_3 layers are grown reliably and reproducibly on thermally oxidized Si-wafers at deposition rates of 2-4 nm/min. Optical loss of as-deposited planar waveguides as low as 0.11±0.05 dB/cm at 1.5-µm wavelength has been demonstrated. The channel waveguide fabrication is based on BCl_3/HBr chemistry in combination with standard photoresist and lithography processes. Upon process optimization channel waveguides with up to 600-nm etch depth, smooth side walls and optical losses as low as 0.21±0.05 dB/cm have been realized. Rare-earth-ion doping has been investigated by co-sputtering from a metallic Er target during Al_2O_3 layer growth. At the relevant dopant levels (~10^{20} cm^{-3}) lifetimes of the $^4I_{13/2}$ level as high as 7 ms have been measured. Gain measurements have been carried out over 6.4-cm propagation length in a 700-nm-thick Er-doped Al_2O_3 waveguide. Net optical gain has been obtained over a 35-nm-wide wavelength range (1525-1560 nm) with a maximum of 4.9 dB.

Keywords: low-loss waveguide, erbium, aluminum oxide, integrated optics, optical amplifier, reactive co-sputtering

1. INTRODUCTION

Amorphous aluminum oxide (Al_2O_3) is a promising host material for active integrated optical devices such as rare-earth-ion-doped amplifiers and lasers [1]. When comparing the performance of rare-earth-ion-doped dielectric amplifiers and lasers with their semiconductor based counterparts, the former provide potentially higher output powers, less noise, and lower thermal drift. Another advantage of the amorphous Al_2O_3 technology is given by the access to Si-compatible deposition techniques. Due to the amorphous character of the Al_2O_3 host material broad emission linewidths, up to 55 nm around 1.55 µm [1], are feasible. This is particularly attractive for amplifiers in wavelength division multiplexing (WDM) devices and for tunable integrated laser devices.

Over the past decade Al_2O_3 growth processes based on different techniques have been developed by various research groups. Suitable deposition techniques are pulsed laser deposition (PLD) [5][6], atomic layer deposition (ALD) [7][8], chemical vapor deposition (CVD) [9][10], the sol-gel method [11][13], sputtering from dielectric targets [14][15], and reactive co-sputtering from metallic targets [4][16].

In general, thin films for applications in integrated optical devices should fulfill the requirements of low propagation loss, reproducible layer thickness and refractive index over a large substrate area, and sufficiently high deposition rate in order to enable waveguide fabrication up to the µm-thickness range. In case of active device applications based on rare-earth-ion transitions the criterion of OH^--free deposition is an additional requirements, because these bonds induce lifetime quenching and, hence, largely diminish the gain efficiency. When comparing the properties of the applied deposition techniques, it becomes obvious that CVD and sol-gel techniques suffer from OH^- incorporation due to the presence of hydroxyl groups in the process precursors. The application of ALD for optical waveguides, although

resulting in thin films with excellent quality, is limited by its low deposition rate, which results in film thicknesses of only several tens of nanometers. The main draw-back of the PLD technique consists in the limited substrate area (typically 1-3 cm range) which can be covered by a thin film with acceptable uniformity. This size limitation restricts the integration scale of complex integrated optical devices. Based on the results of previous studies, the sputtering technique is promising for the fabrication of amorphous Al_2O_3 films, since it combines an inherently low OH^- content with relatively fast, uniform, and controlled deposition over a large substrate area.

By applying the sputtering process to host material fabrication, the high potential of erbium-doped Al_2O_3 waveguides for integrated optical amplifiers and tunable light sources has been demonstrated [4][17]. However, the fabrication processes and material properties faced several disadvantages. The high propagation loss of as-deposited Al_2O_3 slab waveguides of 20 dB/cm [17] could be optimized to 0.35 dB/cm only after an additional annealing step. The active ions were incorporated by ion implantation, followed by additional annealing steps in order to decrease the implantation damage. This leads to an increase in processing complexity. The lowest background loss of Al_2O_3:Er waveguides of approximately 0.25 dB/cm [4] was obtained by reactive co-sputtering based on DC-driven sputtering guns, however with the drawback of poor process stability and reproducibility owing to varying condition of the sputtering target. Finally, the lack of reliable etching techniques for low-loss channel waveguide fabrication in Al_2O_3 prohibited a breakthrough of active devices based on amorphous Al_2O_3 technology.

In this paper we will describe the optimization of the Al_2O_3 reactive co-sputtering process and report on the fabrication of high-quality channel waveguides. Doping of the optimized Al_2O_3 host material with Er^{3+} ions is studied in detail. Measurements of dopant concentration, luminescent lifetime, absorption and emission cross-sections, and optical gain will be presented.

2. EXPERIMENTAL SET-UP

2.1 Waveguide fabrication

The Al_2O_3 layers were deposited with an AJA ATC 1500 sputtering system. The schematic layout of this equipment is depicted in Figure 1. Substrates of 100-mm size were introduced through a load-lock and fixed on a rotating substrate holder. The substrate can be heated up to a maximum temperature of 800ºC. The temperature of the heating element was controlled within ± 3ºC. The background pressure of the deposition chamber was 10^{-7} mTorr. The chamber pressure during deposition was manually adjusted by a valve to the pump unit and can be regulated within ±0.1 mTorr. The deposition system is equipped with three sputtering guns for 2-inch sputtering targets, which can be driven by either RF or DC power supplies, both having a maximum range of 500 W. The power was typically set within ±1 W. All sputtering guns are connected to an argon gas line with a maximum flow of 100 sccm controlled by flow controllers with an accuracy of 1%. The distance between the substrate holder and the sputtering target can be adjusted within a range of 10 to 18 cm. An oxygen flow controlled with 1% accuracy is connected to a gas inlet tube at the chamber. For Al_2O_3 deposition, a high-purity 2-inch aluminum target was mounted to one of the sputtering guns. The fabrication of rare-earth-ion-doped Al_2O_3 waveguides was carried out with a metallic Er target with 99% purity. The thickness (*d*) and refractive index (*n*) of the layers were measured by a Woollam M44 spectroscopic ellipsometer. In order to calculate the stress of the thin films the wafer bow of the Si wafers was measured over a length of 80 mm before and after layer deposition. By combining data on the change in bow, layer thickness, and substrate specific properties, the stress value was calculated.

For the fabrication of channel waveguides a load-lock equipped Oxford Plasmalab 100 inductively-coupled plasma (ICP) reactive ion etch (RIE) system was applied. The ICP source was controlled by a 3-kW, 13.56-MHz RF generator, while substrate bias was controlled separately by a 600-W, 13.56-MHz RF generator. The Al_2O_3 etching process was based on BCl_3/HBr chemistry [18].

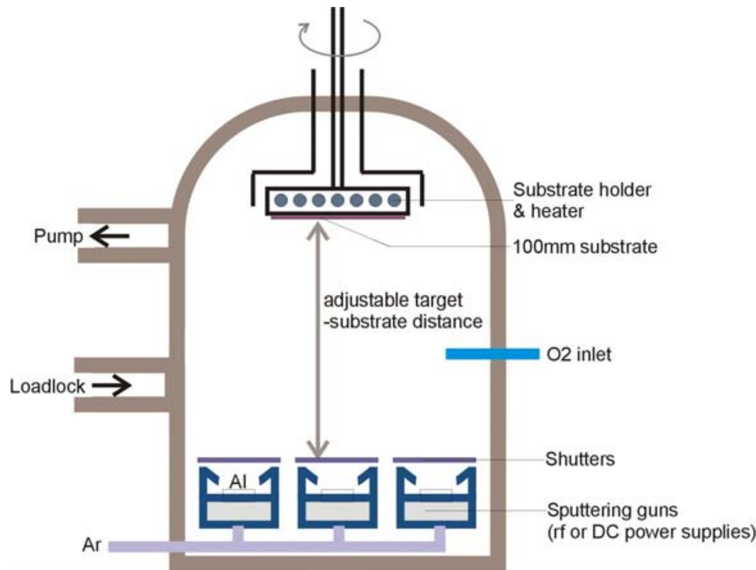

Figure 1: Schematic layout of the deposition equipment for reactive co-sputtering

2.2 Optical characterization

For optical characterization, un-doped and doped Al_2O_3 films were deposited on 100-mm Si wafers, which were thermally oxidized to a thickness of 8 µm. The thickness, refractive index, and their uniformities over the wafer area were measured by a commercial Metricon prism-coupling set-up, which can be operated at four laser wavelengths (633 nm, 830 nm, 1300 nm, and 1550 nm). From the refractive indices determined for both polarizations, TE (n_{TE}) and TM (n_{TM}), the material birefringence given by $\Delta n_{TM\text{-}TE} = n_{TM} - n_{TE}$ was calculated. The optical loss of planar waveguide structures was measured by the moving prism method [19], while for loss measurements in channel waveguides the cut-back method was applied.

For determination of the absorption cross-sections of the erbium-doped planar waveguides the loss spectrum was measured over the wavelength range from 500-1600 nm by applying a white-light source in combination with a spectrometer. The wavelength step-size of the spectral measurement was 1 nm. For the absorption peaks with peak wavelength at 651, 795, 976, 1481, and 1529 nm the background losses were subtracted from the absorption spectra and the absorption cross-sections were calculated.

Lifetime and photoluminescence measurement were carried out at the University of Hamburg and University of Twente, respectively. The luminescent decay curves at 1535 nm were measured upon short-pulse (10-Hz repetition rate, 17-mJ pulse energy) excitation at 797-nm wavelength. The excitation pulse was focused onto the sample surface. After pump-light filtering and dispersion by a monochromator, the optical signal was detected by a Ge-photomultiplier, which was connected to an oscilloscope for data acquisition. The luminescence spectra were measured upon excitation with 150 mW (CW) at 977-nm wavelength from a Ti:sapphire laser. The excitation light was prism-coupled into the planar waveguides. The luminescence signal was collected with a liquid optical fiber and analyzed with an optical spectrometer. From the luminescence spectra and the absorption cross-sections the emission cross-sections were calculated by applying the McCumber method of reciprocity [17][20]. Gain experiments were carried out by pumping Er-doped shallow-etched channel waveguides with varying power (0-100 mW) from a Ti:sapphire laser tuned to 977-nm wavelength. The signal beam (small-signal approximation) was tuned between 1480-1600 nm. The combined pump and signal beams were end-fire coupled into the waveguide channels. After subtracting the optical loss spectrum from the detected amplified signal, the optical gain was obtained over the wavelength tuning range.

3. RESULTS AND DISCUSSION

3.1 Un-doped Al_2O_3 films

In order to optimize the Al_2O_3 layer properties (deposition rate, refractive index, film density, stress, material birefringence, and optical loss), the influence of the various processing parameters (temperature, pressure, power, total flow, and oxygen percentage in flow) was studied. The wide range over which the deposition parameters have been varied is given in Table 1. A detailed discussion on the change of thin-film properties as a function of processing parameters can be found elsewhere [21]. The most important difference between deposition with DC and RF based sputtering was found to be the optical loss in the planar waveguides. For DC-deposited Al_2O_3 waveguides high optical loss (>25 dB/cm) were observed in all layers. This loss is attributed to arcing (power breakthrough events on the oxidized target surface) while depositing with DC driven sputtering guns. Upon arcing large pieces of target material are incorporated in the growing layer, which results in low-quality, porous thin films. During RF-driven sputtering arcing is prevented by the alternating field applied to the targets. Therefore, the latter process is considerably better controlled and high-quality thin films are feasible. In case of the RF-process it was observed that the optical loss of the thin films strongly depends on the substrate temperature (Fig. 2). This behavior can be understood when considering the impact of the temperature on the surface mobility of the ad-atoms.

Table 1. Process parameters for optimization of the Al_2O_3 layer properties upon deposition with DC and RF co-sputtering

Processing parameter	DC sputtering process	RF sputtering process
Temperature *T* [ºC]	400 - 500	350 - 550
Pressure *p* [mTorr]	3 – 5	3 – 6
Distance substrate-target [cm]	14 - 18	18
Power *P* [W]	150 – 275	150 - 250
Total flow [sccm]	11 – 24.5	31.5 - 42
O_2 flow percentage [%]	10 - 25	5 – 10

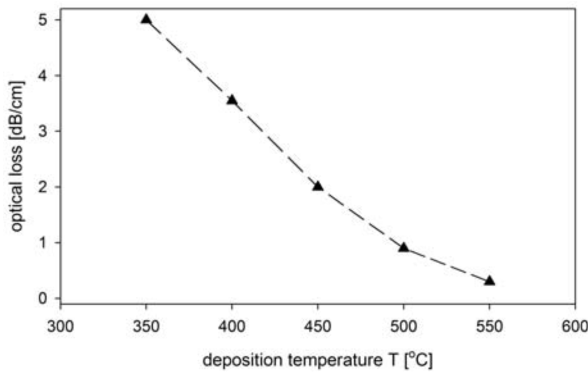

Figure 2: Optical loss at 633-nm wavelength as a function of deposition temperature (RF sputtered Al_2O_3 waveguides)

At deposition temperatures as high as 550ºC, the optical loss of ~700-nm thick Al_2O_3 waveguides is 0.3 dB/cm and 0.1 dB/cm for propagation at 633 nm and 1550 nm, respectively. Based on the loss measurement results, which are indicative of the excellent thin-film quality, the optimized processing parameters were selected: T = 550ºC, P = 200 W, p = 3 mTorr, flow rate = 31.5 sccm with 5% oxygen. The relevant layer properties of waveguides grown under optimized deposition conditions are summarized in Table 2. It can be seen that the layer uniformity is excellent and comparable to properties of thin films obtained by Si-based waveguide technologies, such as CVD-grown silicon nitride and oxynitride waveguides.

Table 2. Layer properties of optimized Al_2O_3 waveguide films

Layer parameter	
Deposition rate R [nm/min]	5
Thickness uniformity [%] (6 x 6 cm^2 area)	± 1.4
Refractive index n at λ=633 nm (TE)	1.659 ± 0.0005
Refractive index uniformity (6 x 6 cm^2 area)	± 2 x 10^{-4}
Material birefringence Δn_{TE-TM}	2 x 10^{-4}
Stress σ [MPa]	- 50 ± 5

3.2 Er-doped Al_2O_3 waveguides

For the deposition of Er-doped films, the power from a second RF-generator was connected to the gun with the Er target. The Er power was varied between 10 and 150 W, while the remaining deposition parameters were kept constant. The Er concentrations were measured with RBS. The Er concentration as a function of sputtering power in the range up to 25 W is shown in Fig. 3. Er concentrations between $2x10^{19}$ cm^{-3} and $4x10^{20}$ cm^{-3} can be achieved at sputtering powers between 10-25 W. At sputtering powers above 25 W, the Er concentration was found to increase rapidly beyond concentration values, which are useful for amplification at 1.5 µm. For the following relevant properties of the active material (lifetime, absorption- and emission cross-section, gain) we will restrict ourselves to this range.

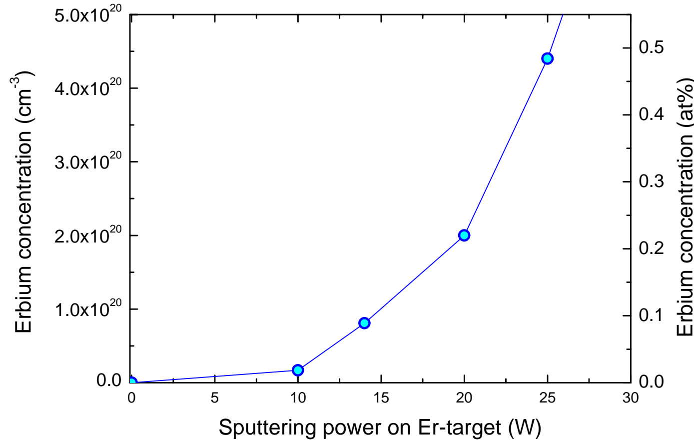

Figure 3. Er concentration of reactively co-sputtered Er: Al_2O_3 as a function of sputtering power on the Er-target

The measured luminescent lifetime of the $^4I_{13/2} \rightarrow {}^4I_{15/2}$ transition (1.5-µm emission) is 7.5 ms, 6.5 ms, 4.6 ms, and 3 ms for Er concentrations of $2x10^{19}cm^{-3}$, $8x10^{19}cm^{-3}$, $2x10^{20}cm^{-3}$, and $4x10^{20}cm^{-3}$, respectively. The long lifetime for lower concentrations compares well with the lifetime of $Al_2O_3:Er^{3+}$ reported in the literature.

For the measured absorption spectra (500-1600 nm wavelength range) of the samples with Er concentrations between $2x10^{19}$ cm^{-3} and $4x10^{20}$ cm^{-3}, the absorption cross-sections $\sigma^{\alpha}(\lambda)$ were calculated by:

$$\sigma^{\alpha}(\lambda) = \frac{\alpha_{Er}(\lambda)}{10\log(e)\ \Gamma(\lambda)\ N_{GS}}, \qquad (1)$$

with $\alpha_{Er}(\lambda)$, the measured loss of the Er-doped film at wavelength λ, N_{GS}, the ground-state population density (approximated by the Er concentration in case of low excitation, and $\Gamma(\lambda)$, the confinement factor of the light beam propagating with wavelength λ in the Er-doped layer.

The absorption cross-sections were calculated for the absorption peaks at 651 nm ($^4F_{9/2}$), 795 nm ($^4I_{9/2}$), 976 nm ($^4I_{11/2}$), 1487 nm and 1530 nm ($^4I_{13/2}$). The absorption cross-sections obtained from our measurements are presented in Table 3 and compared to previously reported values. It can be seen that within the error ranges, our measured absorption cross-sections agree with values previously reported.

Table 3. Comparison of measured absorption cross-sections of Al_2O_3: Er^{3+} layers with literature values

Absorption cross-sections (10^{-21} cm^2)					**ref**
$^4F_{9/2}$	$^4I_{9/2}$	$^4I_{11/2}$	$^4I_{13/2}$	$^4I_{13/2}$	
4.0 ± 0.4 (651 nm)	1.2 ± 0.1 (795 nm)	1.6 ± 0.6 (976 nm)	2.8 ± 0.25 (1481 nm)	5.0 ± 0.7 (1529 nm)	This work
			2.6 (1480 nm)	4.3 (1533 nm)	[4]
4.0 ± 0.7 (652 nm)	< 0.7 (-)	1.7 ± 0.7 (980.5 nm)	3.0 (1480 nm)	5.7 ± 0.7 (1529 nm)	[17][22]

The emission spectrum of the $^4I_{13/2} \rightarrow {}^4I_{15/2}$ was measured upon excitation at 977 nm. Applying the McCumber theory of reciprocity, the emission cross-section $\sigma^e(\nu)$ as a function of photon energy ν was derived from the absorption cross section:

$$\sigma^e(\nu) = \frac{Z_g}{Z_e} \exp\left(\frac{\varepsilon - h\nu}{kT}\right) \sigma^a(\nu), \qquad (2)$$

with T, the temperature, k, Boltzmann's constant, and Z_e and Z_g, the partition functions of the excited and ground state, respectively, which can be approximated by $Z_g/Z_e \sim 1$.

The absorption and emission cross-sections based on averaged values measured in samples with Er concentrations in the range of interest are shown in Fig. 4.

For the gain measurements shallow waveguide channels (~ 20 nm) were etched into the Er-doped films in order to confine pump and signal light over the 6.4-cm propagation length. Previously [18], we had obtained waveguide channels with 220-nm step height with optical losses as low as 0.21±0.05 dB/cm in the 1500-nm wavelength range. Therefore, we assume that any additional loss due to channel fabrication can be neglected in our shallow-etched samples.

The measured absorption (un-pumped) and gain (pumped) spectra over the 1480-1600-nm wavelength range are shown in Fig. 5. Net optical gain has been obtained over a 35-nm wide wavelength range (1525-1560 nm) with a maximum of 4.9 dB (0.76 dB/cm). To the best of our knowledge, this is the highest reported gain value to date.

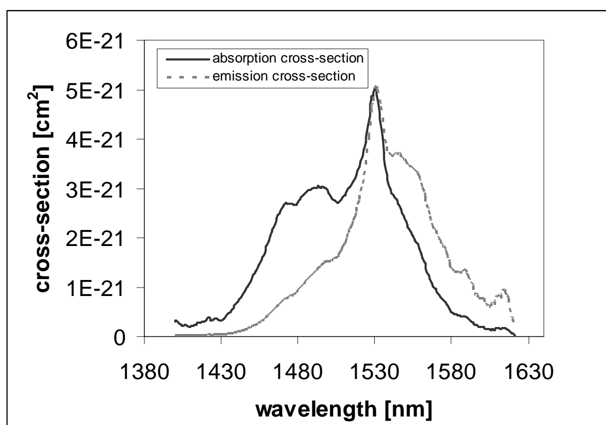

Figure 4. Absorption and emission cross sections of Er-doped waveguides

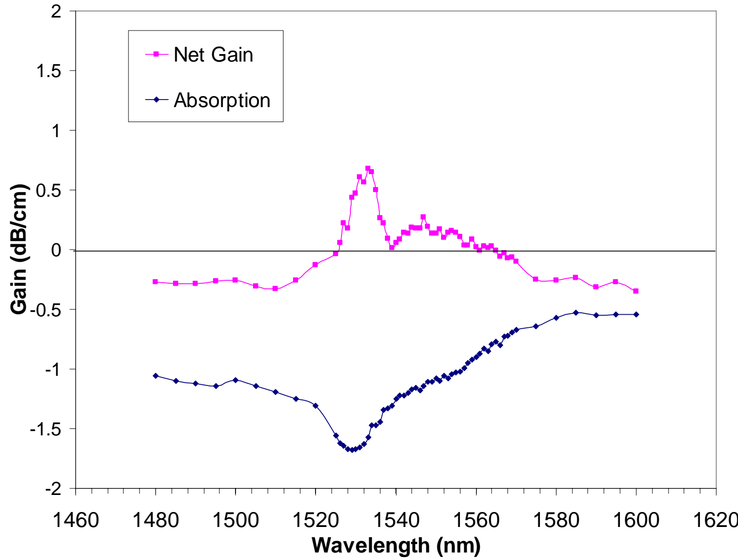

Figure 5. Amplifications spectrum and net gain of an Er-doped Al_2O_3 waveguide with an Er concentration of $9x10^{19}cm^{-3}$

4. CONCLUSIONS

The optical properties of optimized amorphous Al_2O_3 optical waveguides have been presented. As-deposited planar waveguides with optical losses as low as 0.11±0.05 dB/cm at 1.5-µm wavelength have been demonstrated. The optimized deposition process is well-suited for reliable and reproducible fabrication of highly-uniform thin films on 100-mm substrates. Er^{3+}-doped thin films have been fabricated by co-sputtering from a metallic Er target. At dopant concentrations in the range of 10^{19}-10^{20} cm^{-3} lifetimes of the $^4I_{13/2}$ level as high as 7 ms have been measured. Absorption and emission cross-sections have been obtained and found to be in good agreement with values previously reported in the literature. First gain measurements have been carried out on a 6.4-cm long sample. Net optical gain has been obtained over a 35-nm-wide wavelength range (1525-1560 nm) with a maximum of 4.9 dB at 1535 nm.

Future research will focus on detailed spectroscopic studies of $Al_2O_3:Er^{3+}$, gain optimization, and application of Er-doped thin films in integrated optical amplifier devices.

5. ACKNOWLEDGMENTS

The research presented in this paper was financially supported by the European Commission and carried out within the framework of the EU-STREP 017501 project PI-OXIDE.

The authors thank T. van Wijngaarden and W.A. Bik of the Surfaces, Interfaces and Devices group, Debye Institute, University of Utrecht for their support with the RBS measurements.

The authors also thank A. Kahn, H. Scheife, and G. Huber from the Institute of Laser-Physics, University of Hamburg for their support with the lifetime measurements.

REFERENCES

[1] G.N. van den Hoven, R.J.I.M. Koper, A. Polman, C. van Dam, K.W.M. van Uffelen, and M.K. Smit, "Net optical gain at 1.53 μm in Er-doped Al_2O_3 waveguides on silicon," Appl. Phys. Lett. 68, 1886-1888 (1996).

[2] G. N. van den Hoven, E. Snoeks, A. Polman, J.W.M. van Uffelen, Y.S. Oei, and M.K. Smit, "Photoluminescence characterization of Er-implanted Al_2O_3 films," Appl. Phys. Lett. 62, 3065–3067 (1993).

[3] C.E. Chryssou and C.W. Pitt, "Er -doped Al_2O_3 thin films by plasma-enhanced chemical vapor deposition (PECVD) exhibiting a 55-nm optical bandwidth," IEEE J. Quantum Electron. 34, 282–285 (1998).

[4] S. Musa, H.J. van Weerden, T.H. Yau, and P.V. Lambeck, "Characteristics of Er-doped Al_2O_3 thin films deposited by reactive co-sputtering," IEEE J. Quantum. Electron. 36, 1089-1097 (2000).

[5] A. Suarez-Garcia, J. Gonzalo, and C.N. Afonso, "Low-loss Al_2O_3 waveguides produced by pulsed laser deposition at room temperature," Appl. Phys. A 77, 779-83 (2003).

[6] A. Pillonnet, C. Garapon, C. Champeaux, C. Bovier, R. Brenier, H. Jaffrezic, and J. Mugnier, "Influence of oxygen pressure on structural and optical properties of Al_2O_3 optical waveguides prepared by pulsed laser deposition", Appl. Phys. A 69, 735-738 (1999).

[7] Y. Kim, S.M. Lee, C.S. Park, S.I. Lee, and M.Y. Lee, "Substrate dependence on the optical properties of Al_2O_3 films grown by atomic layer deposition," Appl. Phys. Lett. 71, 3604-3606 (1997).

[8] S. Jakschik, U. Schroeder, T. Hecht, D. Krüger, G. Dollinger, A. Bergmaier, C. Luhmann, and J.W. Bartha, "Physical characterization of thin ALD–Al_2O_3 films," Appl. Surf. Sci. 211, 352-359 (2003).

[9] M. Ishida, I. Katakabe, T. Nakamura, and N. Ohtake, "Epitaxial Al_2O_3 films on Si by low-pressure chemical vapor deposition," Appl. Phys. Lett. 52, 1326-1328 (1988).

[10] C.J. Kang, J.S. Chun, and W.J. Lee, "Properties of aluminum oxide films prepared by plasma-enhanced metal-organic chemical vapor deposition," Thin Solid Films 189, 161-173 (1990).

[11] A. Pillonnet-Minardi, O. Marty, C. Bovier, C. Garapon, and J. Mugnier, "Optical and structural analysis of Eu^{3+}-doped alumina planar waveguides elaborated by the sol-gel process," Opt. Mater. 16, 9-13 (2001).

[12] M. Benatsou, B. Capoen, M. Bouazaoui, W. Tchana, and J.P. Vilcot, "Preparation and characterization of sol-gel derived Er^{3+}:Al_2O_3–SiO_2 planar waveguides," Appl. Phys. Lett. 71, 428-430 (1997).

[13] X.J. Wang and M.K. Lei, "Preparation and photoluminescence of Er^{3+}-doped Al_2O_3 films by sol–gel method," Thin Solid Films 476, 41-45 (2005).

[14] M.K. Smit, G.A. Acket, and C.J. van der Laan, "Al_2O_3 films for integrated optics," Electron. Opt. 138, 171-81 (1986).

[15] S.M. Arnold and B.E. Cole, "Ion beam sputter deposition of low loss Al_2O_3 films for integrated optics," Electron. Opt. 165, 1-9 (1988).

[16] B.J.H. Stadler, M. Oliviera, and L.O. Bouthillette, "Alumina Thin Films as Optical Waveguides," J. Am. Ceram. Soc. 78, 3336-44 (1995).

[17] G.N. van den Hoven, J.A. van der Elsken, A. Polman, C. van Dam, K.W.M. van Uffelen, and M.K. Smit, "Absorption and emission cross sections of Er^{3+} in Al_2O_3 waveguides", Appl. Opt. 36, 3338-41 (1997).

[18] J.D.B. Bradley, F. Ay, K. Wörhoff, and M. Pollnau, "Fabrication of low-loss channel waveguides in Al_2O_3 and Y_2O_3 layers by inductively coupled plasma reactive ion etching," Appl. Phys. B 89, 311-318 (2007).

[19] T.H. Hoekstra, Ph.D. thesis, University of Twente, Enschede (1994).

[20] D.E. McCumber, "Einstein relations connecting broadband emission and absorption spectra," Phys. Rev. A 136, 954–957 (1964).

[21] K. Wörhoff, F. Ay, and M. Pollnau, "Optimization of Low-Loss Al_2O_3 Waveguide Fabrication for Application in Active Integrated Optical Devices", ECS Transactions 3 (11), 17-26 (2007).

[22] C. Strohhöfer and A. Polman, "Absorption and emission spectroscopy in Er^{3+}-Yb^{3+} doped aluminum oxide waveguides," Opt. Mater. 21, 705-712 (2003).